Portland State University

PDXScholar

Physics Faculty Publications and Presentations | Physics

10-1-2012

Dark current modeling with a moving depletion edge

Justin Charles Dunlap
Portland State University

Morley M. Blouke
Portland State University

Erik Bodegom
Portland State University

Ralf Widenhorn
Portland State University

Follow this and additional works at: https://pdxscholar.library.pdx.edu/phy_fac

Part of the Physics Commons

Let us know how access to this document benefits you.

Citation Details

"Dark current modeling with a moving depletion edge," Justin C. Dunlap, M. M. Blouke, Erik Bodegom, Ralf Widenhorn, Journal of Electronic Imaging. Vol. 21, Issue 4 (Oct-Dec 2012).

This Article is brought to you for free and open access. It has been accepted for inclusion in Physics Faculty Publications and Presentations by an authorized administrator of PDXScholar. Please contact us if we can make this document more accessible: pdxscholar@pdx.edu.

Dark current modeling with a moving depletion edge

Justin C. Dunlap
Morley M. Blouke
Erik Bodegom
Ralf Widenhorn
Portland State University
Portland, Oregon 97207
E-mail: ralfw@pdx.edu

Abstract. *Within a pixel in a digital imager, generally either a charge-coupled device or complementary metal oxide semiconductor device, doping of the semiconductor substrate and application of gate voltages create a region free of mobile carriers called the depletion region. This region fills with charge after incoming photons or thermal energy raise the charges from the valence to the conduction energy band. As the signal charge fills the depletion region, the electric field generating the region is altered, and the size of the region is reduced. We present a model that describes how this dynamic depletion region, along with the location of impurities, will result in pixels that produce less dark current after being exposed to light and additionally show nonlinear production rates with respect to exposure time. These types of effects have been observed in digital imagers, allowing us to compare empirical data with the modeled data. © 2012 SPIE and IS&T.* [DOI: 10.1117/1.JEI.21.4.043011]

1 Introduction

Dark current, a temperature-dependent source of noise present in pixels of digital imagers such as charge-coupled devices (CCDs), is generated in an image whether or not the shutter is opened or closed, and is thus a limitation on device performance. This source of dark current is caused by electrons thermally excited from the valence to the conduction band in the silicon comprising the pixels. A CCD's pixel architecture is similar enough to a p-n junction of a diode that the pixels' dark current can be understood by studying this architecture.[1–5] Along with lattice defects, the presence of heavy metal impurities such as Cu, Au, Ni, and Fe within the pixels' silicon crystal lattice are responsible for the nonuniform distribution of dark current across the pixels in the imager.[6–10]

The amount of dark current is generally expected to be about the same regardless of whether the imager is exposed to light or left in the dark. However, it was found in prior studies that the dark current generation rate for certain pixels was changed by the presence of illumination.[11] For these pixels, the standard method of removing the dark current is insufficient. In particular, after an image is taken, the standard method of correction involves taking an exposure at the same integration time as the image, except now leaving the shutter closed. This "image" is referred to as a dark frame. With the intention of removing the dark noise present in the original image, the pixel values from this dark frame are subtracted from the original image's pixel values. While more complex methods of correction exist, such as taking multiple dark frames and averaging them to reduce shot noise, they generally all rely on the expectation that the dark noise will be consistent when the shutter is open or closed.

Using the mechanisms described in a previous publication,[12] we present a study on how modeling a moving depletion region in a pixel can duplicate the changes to the dark current generation rate found in imagers in the prior studies when exposed to light, compared to not being exposed.[11] The model assumes the presence of one or more impurities in the pixel that produce a distinctive rate of dark current per impurity. Due to filling with signal charge, the depletion edge of the potential well will shift possibly far enough to shift the impurity out of the well. Minimal amounts of dark current will therefore be collected from this impurity while no longer in the well. Light exposure essentially results in large amounts of signal charge being collected by the well and rapidly shifts the depletion edge. Therefore, it is possible for a pixel with one or more impurities in the region of the depletion edge shift to produce significantly less dark current when exposed to light than when not exposed.

Similarly, although generally slower, thermal excitation of signal charges collected by the well also results in a shrinking depletion region. For pixels with impurities near the depletion edge, the collection rate of dark current from these impurities will decrease with increasing exposure time. The model's ability to duplicate features seen in empirical data due to the thermal excitation versus exposure time has been described in detail elsewhere.[12] However, we present here how these behaviors can be modeled using similar parameters as the response to illumination, and similarities will be compared between the two effects.

2 Dynamic Depletion Edge Model

2.1 *Model Overview*

The modeled pixel consists of a one-dimensional (1-D) depletion region with one or more impurities within the region. Figure 1 shows a two-dimensional (2-D) representation of the (1-D) model. As the depletion well fills with signal charge, the edge of the depletion region, w, contracts and moves closer to the oxide layer. As it contracts, the impurity sits closer to the edge and, depending on the location, may

Paper 12197P received May 24, 2012; revised manuscript received Aug. 10, 2012; accepted for publication Oct. 18, 2012; published online Nov. 13, 2012.
0091-3286/2012/$25.00 © 2012 SPIE and IS&T

Downloaded From: http://electronicimaging.spiedigitallibrary.org/ on 03/08/2013 Terms of Use: http://spiedl.org/terms

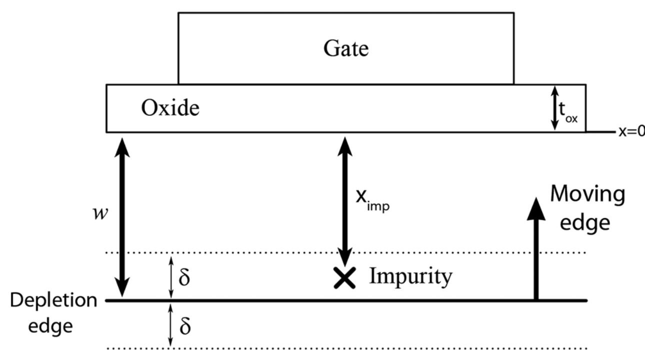

Fig. 1 Two-dimensional representation of the one-dimensional pixel with an impurity near the moving depletion edge.

ultimately no longer be located within the depletion region. When this occurs, the pixel will no longer collect the majority of the thermally generated electrons from the impurity. We have added a region, defined by plus or minus δ from the depletion edge, where there is a probability that either thermally generated electrons will escape the depletion region when the impurity sits within the depletion region, or a probability that thermally generated electrons will be collected by the depletion well when the impurity sits just outside the depletion edge.

We have previously allowed signal charge to be accumulated slowly to model pixels' dark current response to a gradual collection of dark signal, simulating a relatively long-exposure dark frame.[12] Now, we present data where we allowed the pixels to not only gradually accumulate signal charge during a relatively long-exposure dark frame, but additionally provided a large initial signal charge to simulate an exposure to a flash of light during the beginning of the integration time. These conditions simulate a study where dark frames were taken both after a large flash of light and without the flash of light. Integration time of the dark frame as well as initial signal charge are variables that can be chosen by the user, whereas the rest of the values were chosen to be consistent with representative values found for typical imagers. The parameters used by the model are summarized in Table 1. When using these values, the depletion edge starts at a distance of 5.33 μm from the oxide layer, and moves to 3.93 μm when the depletion region is entirely filled with signal charge.

Table 1 Modeling parameters.

Name	Parameter	Value chosen
Gate voltage	V_g	−5 V
Buried channel implant dose	Q_{cd}	2.5×10^{12} cm^{-2}
Oxide thickness	t_{ox}	7.2×10^{-6} cm
Number of acceptors per volume	N_a	5.0×10^{14} cm^{-2}
Relative oxide permittivity	$\varepsilon_{ox}/\varepsilon_0$	3.9
Relative semiconductor permittivity	$\varepsilon_{Si}/\varepsilon_0$	11.7
Range	r	1.0×10^{-5} cm
Straggle	σ	3.0×10^{-5} cm
Camera gain	g	3.0 e-/DN
Rate of dark current without impurity	R_0	1.0 DN/s
Rate of additional dark current due to a single impurity	R_1	10.0 DN/s
Pixel collection area	A	2.1×10^{-7} cm^2
Total pixels	N_{pix}	1×10^6
Full well count		65,536 DN (16 bit)
Number of impurities	N_{imp}	50,000 impurities
Delta edge	δ	5.0×10^{-6} cm
Integration time		500 s
Initial signal charge		30,000 counts

2.2 *Modeled Response to Illumination*

To get an overview of the effect of illumination, or an initial partial filling of the potential well, we define ΔD_{Light}:

$$\Delta D_{\text{Light}} = D_{NL} - D_L, \tag{1}$$

where D_{NL} is the total number of dark counts generated with no initial signal charge in the potential well for a given integration time, and D_L is the total number of dark counts generated for the same integration time after the initial signal charge is added. In practice, this initial signal charge could be added by exposing the imager to an initial flash of light prior to the longer exposure time where only dark current is collected.

A 2-D distribution of the loss in dark count, ΔD_{Light}, versus the dark-count level, D_{NL}, was created using this model. The ΔD_{Light} versus D_{NL} plane was divided into intervals of size 250×250 DN, and the shades of gray represent the logarithm of the number of pixels in a specific interval. Figure 2 represents this distribution for modeled data using the parameters given in Table 1. Varying the parameters, such as DC generation rate, or initial signal charge, will result in variations in the data and the graph. Extensive discussion on the generation of these type of graphs can be found in previous publications.[11–13]

A pixel with a single impurity that remains fully within the depletion region for the entire collection time without exposure to light will have a D_{NL} of about 5500 DN. If, additionally, the impurity remains fully within the depletion region during the collection time after the initial flash, the impurity will produce just as much dark current and will have a ΔD_{Light} value of about 0. However, if the initial flash of light moves the depletion edge past the impurity, the pixel will collect no dark current from the impurity, and the pixel will have a ΔD_{Light} of about 5500. If the depletion edge moves past the impurity at some point during the collection time after the exposure of light, the pixel will lie in the grouping of pixels parallel to the y-axis at about 5500 DN.

Downloaded From: http://electronicimaging.spiedigitallibrary.org/ on 03/08/2013 Terms of Use: http://spiedl.org/terms

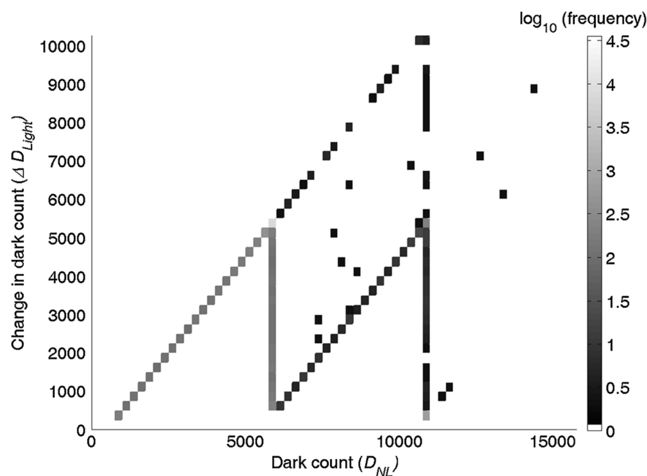

Fig. 2 Change of dark count after illumination versus dark count of a 500 s dark frame with an initial count of 30,000.

Now, if the impurity lies close enough to the depletion edge such that it is partially or fully removed from the depletion region during the collection time without exposure to light, the pixel will have a D_{NL} value less than 5500 DN. Of course, the impurity will also be removed from the depletion region by the exposure to light or during the subsequent collection time after the exposure, so the pixel will have a small or zero D_L value, and ΔD_{Light} will be about the same value as D_{NL}.

A pixel with two impurities that remain fully within the depletion region during the collection time with no exposure to light will have a D_{NL} of about 11,000 DN. If both those impurities are also fully within the depletion region for the entire collection time after the flash, the pixel will again produce just as much dark current and will have a ΔD_{Light} value of about 0. If both impurities are fully removed from the depletion region by the flash, the pixel will produce no dark current for the collection period, giving a D_L value of 0, and ΔD_{Light} will also be about 11,000 DN. If just one impurity is removed from the collection region by the flash while the other remains fully within the region for the entire collection time, the D_L value will be about 5500 and thus the ΔD_{Light} value will also be about 5500. If one or both impurities are removed from the collection region during the collection time after the flash, the pixel will lie in the grouping parallel to the y-axis.

For the cases where one or both impurities are partially removed from the collection region during the collection time with no exposure to light, D_{NL} will have values less than 11,000 DN. During or after the flash, if one impurity stays fully within the collection region while the other is removed, D_L will have a value between 5500 and 11,000, and therefore ΔD_{Light} will be between 0 and 5500, approximately the same as D_{NL} for that pixel. If both pixels are removed from the depletion region during or after the flash, D_L will be between 0 and 5500. If both impurities are turned off during the flash, ΔD_{Light} will be approximately the same as D_{NL}. However, if one of the impurities is removed from the depletion region only in the collection time after the flash, the pixel will lie between the two diagonal lines with a D_{NL} value between 5500 and 11,000.

Additionally, with the total number of impurities we use in the model, individual pixels with more impurities of this type are possible but become statistically unlikely. There are a few pixels with three impurities that can be seen in Fig. 2 with D_{NL} values greater than 11,000.

2.3 *Modeled Nonlinear Behavior*

As previously reported,[12] a similar effect can be observed solely due to signal charge generated by dark current. Pixels are typically not only expected to have a linear response to light but also to dark current generated versus time. As such, to get an idea of the linear behavior of the pixels, a linear fit is calculated for dark current generation rates at low exposure times:

$$D_{\text{fit}} = mt, \tag{2}$$

where t is the time, and m is the slope of the fit at low exposure values. To generate Fig. 3, we have used the model to generate dark noise for exposure time values from 5 to 50 s and performed a linear fit on these exposure times. This linear fit can be extrapolated out to arbitrarily longer exposure times, t_0, to calculate the difference, ΔD, between the predicted generated dark noise, $D_{\text{fit}}(t_0)$, compared to the actual modeled noise, $D(t_0)$:

$$\Delta D = D_{\text{fit}}(t_0) - D(t_0) = mt_0 - D(t_0). \tag{3}$$

Figure 3 is representative of the graphs generated using this method and using the values for the parameters given in Table 1. Additionally, t_0 is chosen to be 1800 s. The x-axis is now the slope, m, and the y-axis is ΔD.

Figure 3 appears to share general features with the graphs generated with the simulated moving depletion edge due to an initial exposure to light. Discussion on the location of pixel impurities and where they would end up on the graph is similar to the discussion in Sec. 2.2 and discussed more in depth in a previous publication.[12]

3 Discussion

The observed results from the model correspond to many features seen in similar plots of experimental data for existing cameras. Two cameras displaying these behaviors are the

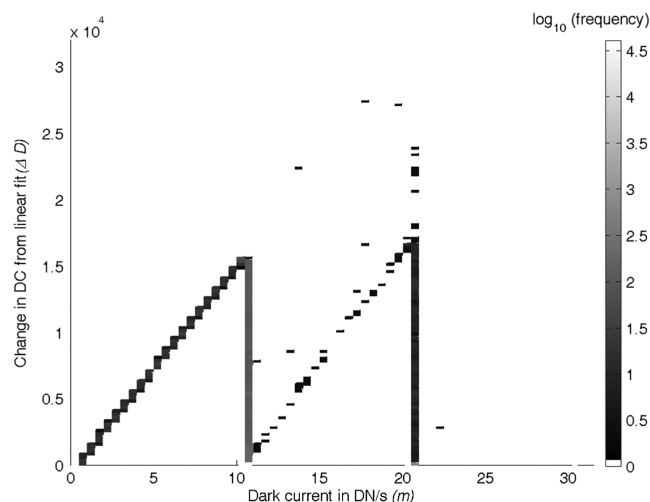

Fig. 3 Modeled dark current for 1×10^6 pixels from a linear fit over the first 50 s versus the change in dark count, ΔD, evaluated at 1800 s.

Downloaded From: http://electronicimaging.spiedigitallibrary.org/ on 03/08/2013 Terms of Use: http://spiedl.org/terms

SBIG ST-8XE with a KAF-1602E CCD sensor and a Meade Pictor 416XT with a Kodak KAF-0400 CCD chip. A previous publication[11] included figures similar to those in Fig. 2, where exposures were taken to highlight the effects discussed above. Using the settings listed in Table 1, except as noted in this paragraph, the model was used to generate graphs matching the actual experimental data. The KAF-1602E has 1.56×10^6 pixels and a gain of 2.3 e-/count, while the KAF-0400 has 3.93×105 pixels and a smaller gain of 1.2 e-/count; these values were used for N_{pix} and g, respectively. Data were taken at 288 K for the KAF-1602E and at 278 K for the KAF-0400. Based on dark current production for a standard pixel with very little dark current production at these temperatures, R_0 was taken to be 0.5 DN/s for both imagers, and based on dark-frame histograms for the peak of hot pixels in the imager; we used 9.5 DN/s for R_1 for the KAF-1602E and 9.0 DN/s for the KAF-0400. N_{imp} was chosen to be 20,000 impurities for the KAF-1602E and 50,000 impurities for the KAF-0400. These values were chosen to generate approximately the same number of pixels as seen in the peak of pixels at about 6000 DN in Figs. 4(a) and 5(a), respectively. A δ value of 3.0×10^{-6} cm provided for the best fit for the data groupings for the KAF-1602E, and a value of 5.0×10^{-6} cm provided for the best fit for the groupings for the KAF-0400. This value is empirically chosen for the two imagers, and our model does not attempt to explain the differing values; they may depend on such factors as the doping concentration. For the graphs from the previous publications, groupings were boxed and labeled for ease of discussion, and we have left the boxes in these figures as well as superimposing them in the modeled data for comparison.

3.1 *SBIG ST-8XE*

Shown in Fig. 4(a) is the change in dark count after illumination versus dark count of a 600 s dark frame after an exposure to light leading to an average value of 26,000 DN across the imager. These values were chosen as the integration time and initial signal, respectively, for the modeled data seen in Fig. 4(b).

For many of the features, there is agreement between experimental and modeled data. In particular, the major groupings of pixels seen at a dark count of about 6000 in Fig. 4(a), those seen in the vertical groupings above these values, and those seen at a diagonal connected to the top of those vertical groupings, are all present in the experimental as well as the modeled data. All of these pixels can therefore be explained by a pixel having a particular type of impurity that generates dark current at a rate of about 9.5 DN/s. The location of the pixel in the graphs will depend on what the depth of the impurity is compared to the quantity of signal charge accumulated in the various exposures used to create the graphs. In addition, there is evidence in the experimental data of groupings seen, due to pixels with two impurities including the extension of the diagonal grouping past the vertical grouping at about 10 DN/s.

Experimental data using the SBIG camera used to generate graphs similar to Fig. 3 are not shown here; however, the model shared a similar success in predicting locations of groupings as seen in the graphs for the exposure to illumination in Fig. 4.

While not sufficient to explain all of the features seen in the experimental data, such as the groups of pixels off the main diagonals (with the greatest slope) and the specific number of pixels seen in each of these groupings, many of the features are captured. The deficiencies of the model are likely due to the model being essentially only (1-D), whereas a more complete model would require analyzing the change in the shape of the three-dimensional (3-D) depletion region. In addition, our model assumes a uniform distribution of impurities as a function of depth within the pixel; however, there may be processes that result in a more systematic location of impurities. A larger percentage of impurities within the region of the depletion edge variation will result in a greater number of pixels in the labeled groups in the experimental data. In addition, a (3-D) model in which the depletion edge moves significantly nearer to the edges of the pixel

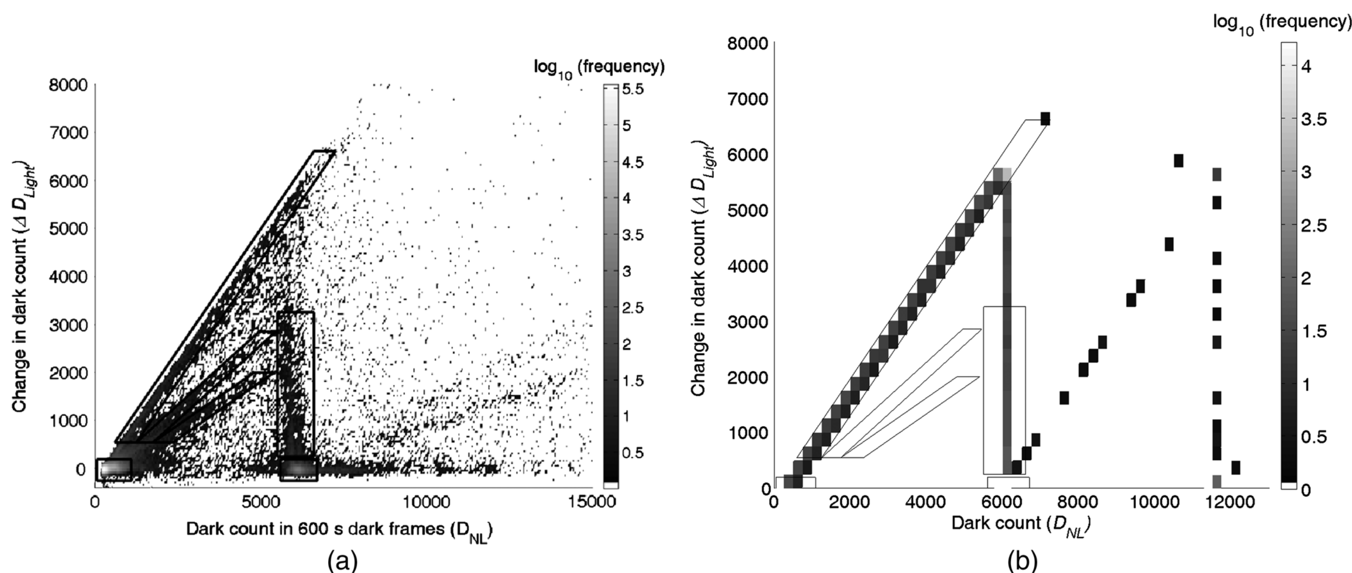

Fig. 4 Change of dark count after illumination versus dark count of a 600 s dark frame. (a) SBIG ST-8XE for an average initial count due to the light exposure of approximately 26,000 at 288 K.[11] (b) Modeled data.

Downloaded From: http://electronicimaging.spiedigitallibrary.org/ on 03/08/2013 Terms of Use: http://spiedl.org/terms

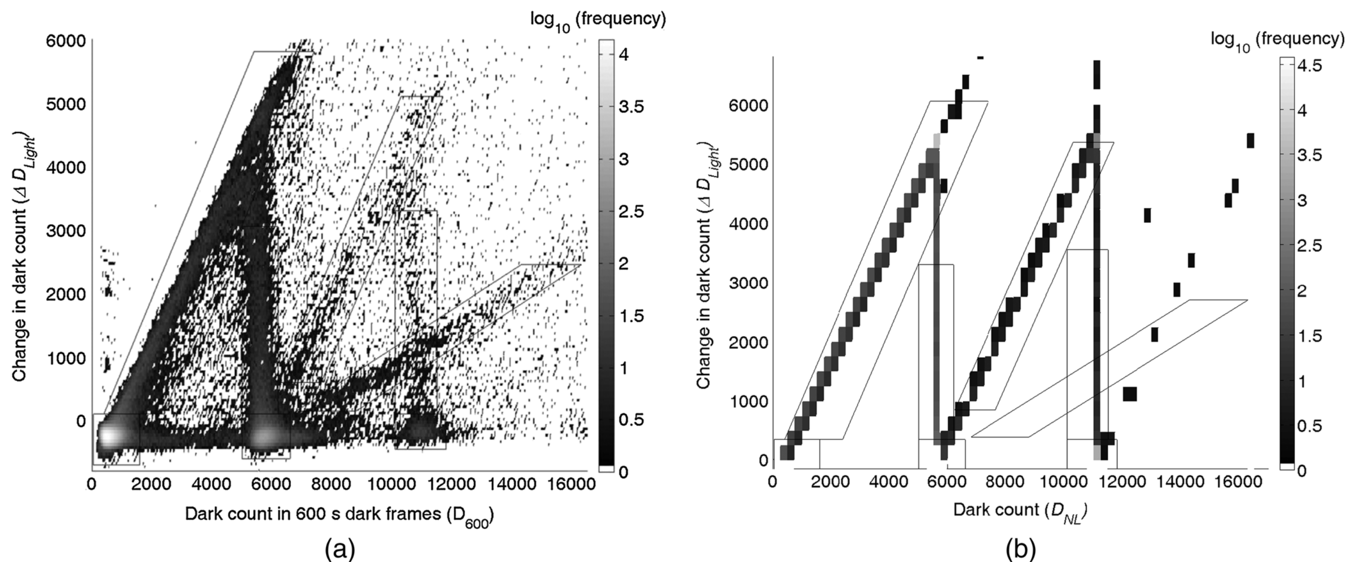

Fig. 5 Change of dark count after illumination versus dark count of a 600 s dark frame. (a) Meade Pictor 416XT for an average initial count due to the light exposure of approximately 42,000 at 278 K.[11] (b) Modeled dark current.

may result in more pixels affected by a similar type of nonlinearity. One possible explanation for more impurities in this region of greater change would be impurities introduced in building the channel stops. Inclusion of these considerations is an area for future work.

3.2 *Meade Pictor 416XT*

Shown in Fig. 5(a) is a similar graph for the Meade imager system, where the change in dark count after illumination is plotted versus dark count of a 600 s dark frame after an exposure to light leading to an average value of 42,000 DN across the imager. These values were chosen as the integration time and initial signal, respectively, for the modeled data seen in Fig. 5(b).

Again, agreement in the features is seen in the graphs of the experimental and modeled data. Due to the relatively larger number of impurities seen in the KAF-0400, there is a second triangle of data seen with larger dark counts along the x-axis. This feature is due to more pixels that have a higher likelihood of having two impurities. Thus, all of the features seen in Fig. 5(b) can be explained by a pixel having one or more impurities with a rate of production at 9.0 DN/s. There exists a grouping starting at about 6000 counts and 0 $\Delta D_{\mathrm{Light}}$ that extends diagonally in the graph to 18,000 counts and a $\Delta D_{\mathrm{Light}}$ of about 3000 that is not explained by the model. This grouping shares similarities with the unexplained groupings in the SBIG 8XE imager.

4 Conclusion

Dark current generation rates that change with exposure to illumination, compared to no exposure, can be reproduced using a model of a (1-D) depletion well with a moving depletion edge and containing one or more impurities near the edge. Additionally, the same behavior of a moving depletion edge is shown to be a mechanism of nonlinear collection rate of dark current. Control of the variables in the model allows for accurately predicting the amount of dark current generated by a pixel as the depletion well is filled with signal charge. The distinctive patterns and groupings seen in multiple camera systems when dark current generation rates are compared in the presence or absence of light are duplicated by this model.

References

1. S. M. Sze, *Physics of Semiconductor Devices*, 2nd ed., John Wiley & Sons, New York (1981).
2. A. S. Grove, *Physics and Technology of Semiconductor Devices*, John Wiley & Sons, New York (1967).
3. R. N. Hall, "Electron-hole recombination in germanium," *Phys. Rev.* **87** (2), 387–388 (1952).
4. C. T. Sah, R. N. Noyce, and W. Shockley, "Carrier generation and recombination in p-n junction and p-n junction characteristics," *Proc. IRE* **45**(9), 1228–1248 (1957).
5. W. Shockley and W. T. Read, "Statistics of the recombination of holes and electrons," *Phys. Rev.* **87**(5), 835–842 (1952).
6. R. D. McGrath et al., "Counting of deep-level traps using a charge-coupled device," *IEEE Trans. Electron Dev.* **34**(12), 2555 (1987).
7. R. Widenhorn et al., "Temperature dependence of dark current in a CCD," *Proc. SPIE* **4669**, 193 (2002).
8. W. C. McColgin et al., "Dark current quantization in CCD image sensors," *Int. Electron Device Meeting 1992*, Vol. 113, pp. 13–16, IEEE, New Brunswick, NJ (1992).
9. W. C. McColgin, J. P. Lavine, and C. V. Stancampiano, "Probing metal defects in CCD image sensors," *Mater. Res. Soc. Symp. Proc.* **378**, 713 (1995).
10. W. C. McColgin et al., "Deep-level traps in CCD image sensors," *Mater. Res. Soc. Symp. Proc.* **510**, 475 (1998).
11. R. Widenhorn et al., "Influence of illumination on dark current in charge-coupled device imagers," *J. Electron. Imaging* **18**(3), 033015 (2009).
12. J. C. Dunlap et al., "Modeling nonlinear dark current behavior in CCDs," *IEEE Trans. Electron Devices* **59**(4), 1114–1122 (2012).
13. R. Widenhorn, J. C. Dunlap, and E. Bodegom, "Exposure time dependence of dark current in CCD imagers," *IEEE Trans. Electron Dev.* **57**(3), 581–587 (2010).

Justin C. Dunlap received his BA degree from the University of California, Berkeley, in physics and astrophysics in 2002. He received his MS degree from Portland State University in physics in 2009. He is currently working toward his PhD at Portland State University, where he researches dark current and digital imagers while also working with undergraduate students to develop a physics curriculum.

Downloaded From: http://electronicimaging.spiedigitallibrary.org/ on 03/08/2013 Terms of Use: http://spiedl.org/terms

Morley M. Blouke received his BS degree from Union College in Schenectady, New York in 1963, and his MS and PhD degrees in physics from the University of Illinois at Urbana-Champaign in 1965 and 1969, respectively. From 1969 to 1982, he was with Texas Instruments, Dallas, Texas, where he worked first in the Semiconductor Research and Development Laboratory, the IR detector group, and finally as a member of the technical staff, the Central Research Laboratory where he developed the CCDs for the first Hubble Wide Field/Planetary Camera. In 1982, he moved to Tektronix, Beaverton, Oregon, as a principal scientist, where he continued to develop large-area, thinned CCDs for scientific and astronomical applications. In 1993, he helped to found Scientific Imaging Technologies as director of technology and continued developing large-area, thinned image sensors. In 2003, he joined Ball Aerospace, Boulder, Colorado, as a staff consultant working in the area of detectors. He retired from Ball in 2009 and now works part time with the detector group at Portland State University in Portland, Oregon.

Erik Bodegom completed his engineering degree at Technical University Delft (Netherlands) and his PhD (1982) at Catholic University of America in Washington, DC. Since 1985, he has been with Portland State University, where he is a professor in the department of physics. His pedagogical activities have included writing a set of astronomical exercises, the development of a resistance probe for use in schools, and the development of software to remotely control observatories. He has served as president of the Oregon Academy of Science. His research activities have ranged from low temperature physics to statistical mechanics and solid-state physics. Over the last decade, his work has focused on the use and understanding of digital imagers.

Ralf Widenhorn did his undergraduate work at the University of Konstanz. He received his MS in physics in 2000 and his doctorate in environmental sciences and resources/physics in 2005, both from Portland State University. He has worked with digital sensors since 1998 and published numerous papers on digital imagers. He is currently a researcher and professor at Portland State University. Besides his work on semiconductor physics his educational activities include biomedical applications of physics.

Downloaded From: http://electronicimaging.spiedigitallibrary.org/ on 03/08/2013 Terms of Use: http://spiedl.org/terms